

LongVie 2: Multimodal Controllable Ultra-Long Video World Model

Jianxiong Gao¹, Zhaoxi Chen³, Xian Liu⁴, Junhao Zhuang⁵, Chengming Xu¹
 Jianfeng Feng¹, Yu Qiao⁶, Yanwei Fu^{1,†}, Chenyang Si^{2,†}, Ziwei Liu^{3,†}
¹FDU, ²NJU, ³NTU, ⁴NVIDIA, ⁵THU, ⁶Shanghai AI Laboratory
<https://vchitect.github.io/LongVie2-project/>



Figure 1. **LongVie 2** is a controllable ultra-long video world model that autoregressively generates videos lasting up to 3–5 minutes. It is driven by world-level guidance integrating both dense and sparse control signals, trained with a degradation-aware strategy to bridge the gap between training and long-term inference, and enhanced with history-context modeling to maintain long-term temporal consistency.

Abstract

Building video world models upon pretrained video generation systems represents an important yet challenging step toward general spatiotemporal intelligence. A world model should possess three essential properties: controllability, long-term visual quality, and temporal consistency. To this end, we take a progressive approach—first enhancing controllability and then extending toward long-term, high-quality generation. We present **LongVie 2**, an end-to-end autoregressive framework trained in three stages: (1) Multi-modal guidance, which integrates dense and sparse control signals to provide implicit world-level supervision and **improve controllability**; (2) Degradation-aware training on the input frame, bridging the gap between training and long-term inference to maintain **high visual quality**; and (3) History-context guidance, which aligns contextual information across adjacent clips to **ensure temporal consistency**. We further introduce **LongVGenBench**, a comprehensive

benchmark comprising 100 high-resolution one-minute videos covering diverse real-world and synthetic environments. Extensive experiments demonstrate that **LongVie 2** achieves state-of-the-art performance in long-range controllability, temporal coherence, and visual fidelity, and supports continuous video generation lasting up to **five minutes**, marking a significant step toward unified video world modeling.

1. Introduction

Recent breakthroughs in video generation have been largely driven by the availability of large-scale datasets and the rapid development of diffusion-based architectures [11, 18, 32, 33, 55]. These advances have enabled powerful models such as CogVideoX [43], HunyuanVideo [36], Kling [37], Sora [31], and Wan2.1 [40] to synthesize photorealistic and semantically rich videos directly from text prompts, demonstrating

that diffusion models can effectively capture both visual dynamics and high-level semantic structures.

Building upon this foundation, research has recently shifted from merely generating visually appealing clips to modeling the underlying dynamics of the physical world. This shift has led to the emergence of video-based world models that simulate realistic environments and interactions, exemplified by HunyuanGameCraft [24], Yume [29], and Matrix-Game [16]. These models incorporate controllable elements—such as camera motion or agent actions—to emulate how the world evolves over time. However, despite these advances, current world models face two major challenges. First, their controllability remains limited, often restricted to low-level or localized adjustments rather than global, semantic-level control over the environment. Second, their temporal scalability is fragile—when extended to long horizons (*e.g.* beyond one minute), these models often exhibit visual degradation and temporal drift, as shown in Fig. 2, where visual quality collapses over time.

Toward the next generation of video world models, we seek to unify two complementary objectives—fine-grained controllability and long-term coherence—within a single framework. An ideal world model should not only generate visually and temporally consistent videos but also respond coherently to structured inputs and interactions. In essence, it should achieve: (1) **Comprehensive controllability**, ensuring that the entire evolving scene remains semantically interpretable and manipulable across time; (2) **Long-term fidelity**, maintaining visual quality over extended sequences; and (3) **Long-context consistency**, preserving stable, realistic dynamics aligned with real-world behavior.

In this paper, we investigate how to construct video world models by extending pretrained video diffusion backbones into controllable long-horizon generators. Introducing controllability into these pretrained architectures is relatively straightforward, as most short-clip diffusion models already support modular conditioning through components such as LoRA [20], ControlNet [52], or similar plug-in adapters. Leveraging this property, we adopt a control-first, then long strategy: we first enhance controllability within short video generation and then progressively extend the temporal horizon to achieve long-range coherence.

Accordingly, we extend controllable short-video generators into long-horizon, temporally coherent frameworks, marking an essential step toward general-purpose video world modeling. To this end, we propose LongVie 2, a controllable long video generation framework built upon an autoregressive paradigm. LongVie 2 is trained through three progressive stages that jointly enhance controllability, temporal consistency, and visual fidelity: **1) Multi-modal guidance** integrates dense (*e.g.*, depth maps) and sparse (*e.g.*, keypoints) control signals under balanced training, providing complementary structural and semantic constraints that offer



Figure 2. **Unstable long-term generation.** As the generated duration increases, current video world models gradually lose controllability, visual fidelity, and temporal consistency.

implicit world-level guidance. **2) Degradation-aware training** introduces controlled degradations to guided frames, effectively bridging the gap between training and long-horizon inference. **3) History context guidance** leverages preceding frames as contextual inputs to maintain long-range consistency across adjacent clips. Together, these stages enable LongVie 2 to generate minute-long controllable videos with strong temporal coherence and high visual fidelity, marking a crucial step toward unified and scalable video world models.

To evaluate the effectiveness of **LongVie 2**, we construct **LongVGenBench**, a benchmark consisting of 100 high-quality videos, each lasting at least one minute. The dataset covers a wide range of scenarios, including both real-world environments and game-based scenes, spanning day and night as well as indoor and outdoor settings, ensuring rich variations in content, structure, and motion dynamics. We compare LongVie 2 and baselines on LongVGenBench in terms of long-term visual quality and temporal consistency. Experimental results demonstrate that LongVie 2 achieves state-of-the-art performance in controllable long video generation, producing videos both temporally coherent and visually realistic.

Our main contributions are summarized as follows:

- We present **LongVie 2**, a controllable long video generation framework that extends pretrained diffusion backbones toward video world modeling.
- We design a **three-stage progressive training scheme** that integrates multi-modal guidance, degradation-aware learning, and history context guidance to enhance controllability, temporal coherence, and visual fidelity, aligning with essential capabilities required for video world models.
- We establish **LongVGenBench**, a benchmark of 100 one-minute videos for evaluating controllability, consistency, and perceptual quality in long video generation.

2. Methodology

Preliminary: Diffusion Models. Diffusion models are powerful video world learners that synthesize realistic videos by progressively removing noise. So, the model ϵ_θ learns to undo a process that adds noise to data. During training, it is

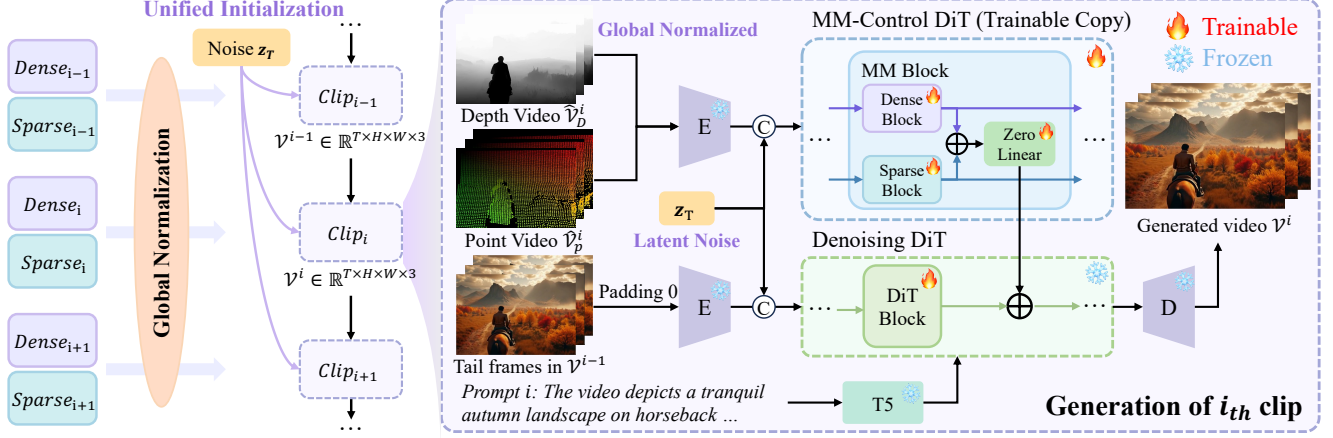


Figure 3. **Framework of LongVie 2.** LongVie 2 serves as a controllable video world model that integrates both dense and sparse control signals to provide world-level guidance for enhanced controllability. A degradation-aware training strategy improves long-term visual quality, while tail frames from preceding clips are incorporated as historical context to maintain temporal consistency over extended durations.

trained to predict the noise added at each step:

$$\mathcal{L} = \mathbb{E}_{\mathbf{x}, \epsilon \sim \mathcal{N}(0,1), t} \left[\|\epsilon - \epsilon_\theta(\mathbf{x}_t, t)\|_2^2 \right], \quad (1)$$

where \mathbf{x}_t , ϵ , \mathbf{x}_0 denote the noisy data at time t , the true noise, and the original data, respectively. To save computing power, Latent Diffusion Models [33] work in a smaller, compressed space. An autoencoder turns \mathbf{x} into a latent code $z = \mathcal{E}(\mathbf{x})$, and the model learns to predict noise in z_t .

Overview. To address the aforementioned challenges and advance toward a unified video world model, we propose LongVie 2, an end-to-end framework trained through three progressive stages, as illustrated in Fig. 3. In Stage I, we inject multi-modal control signals into the model following the standard ControlNet paradigm, enabling implicit world-level guidance that enhances controllability. In Stage II, we introduce a first-frame degradation strategy that simulates long-form deterioration during training, effectively mitigating visual degradation in long-horizon generation. In Stage III, we incorporate historical frames as RGB guidance, allowing the model to leverage temporal context and maintain coherence across adjacent clips.

2.1. Multi-Modal Control Injection

Specifically, we adopt depth maps as dense control signals and point maps as sparse control signals, leveraging the detailed structural information provided by depth and the high-level semantic cues captured by point trajectories to form an implicit world representation. To construct the point map sequences, we follow the procedure in DAS [13], where a set of keypoints is tracked across frames and colored according to their corresponding depth values.

Inspired by the ControlNet [52] architecture, we build our Multi-Modal Control DiT by duplicating the initial 12 layers of the pre-trained Wan DiT and incorporating multi-modal

conditioning inputs while keeping the base model frozen. Specifically, we freeze the parameters θ of the original DiT blocks and construct two trainable branches, each corresponding to a distinct control modality: dense and sparse. These branches, denoted as $\mathcal{F}_D(\cdot; \theta_D)$ and $\mathcal{F}_P(\cdot; \theta_S)$, are lightweight copies of the original DiT layers with parameters θ_D and θ_P , respectively. Each processes the corresponding encoded control signal \mathbf{c}_D or \mathbf{c}_P . To integrate the control branches into the base generation path, we adopt zero-initialized linear layers ϕ^l . These layers allow the control signals to be injected additively into the main generation stream without affecting the model’s initial behavior, as they output zero at the start of training. The overall computation in the l -th controlled DiT block is defined as:

$$z^l = \mathcal{F}^l(z^{l-1}) + \phi^l(\mathcal{F}_D^l(\mathbf{c}_D^{l-1}) + \mathcal{F}_S^l(\mathbf{c}_S^{l-1})), \quad (2)$$

where \mathcal{F}^l is the frozen base DiT block, and \mathcal{F}_D^l , \mathcal{F}_P^l are the control-specific sub-blocks.

While multi-modal control offers the potential for richer and more accurate video generation, simply combining dense and sparse control signals does not guarantee improved performance. In practice, we observe that dense signals tend to dominate the generation process, often suppressing the semantic and motion-level guidance provided by sparse signals. This imbalance can lead to suboptimal visual quality, particularly in scenarios requiring high-level semantic alignment over time. To address this issue, we propose a degradation-based training strategy designed to regulate the relative influence of dense control signals and encourage more balanced utilization of both modalities. This strategy weakens the dominance of the dense input through controlled perturbations at both the feature and data levels:

1) *Feature-level degradation:* During training, with probability α , we randomly scale the latent representation of the dense control by a factor λ sampled uniformly from $[0.05, 1]$.

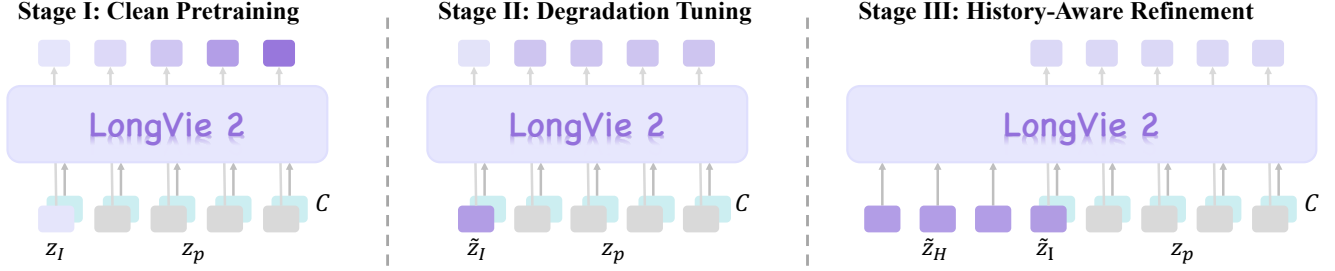


Figure 4. **Training pipeline of LongVie 2.** We first train the model using a standard ControlNet-based pipeline. In the second stage, we introduce degradation to the first frame to bridge the domain gap between ground truth and generated frames. Finally, to ensure temporal consistency, we incorporate historical frame information.

Accordingly, Equation 2 can be reformulated as:

$$z^l = \mathcal{F}^l(z^{l-1}) + \phi^l(\lambda \cdot \mathcal{F}_D^l(c_D^{l-1}) + \mathcal{F}_P^l(c_P^{l-1})), \quad (3)$$

This operation reduces the magnitude of the dense features, making the model more reliant on complementary information provided by the sparse modality. Over time, this encourages the network to learn a more balanced integration of both control sources.

2) *Data-level degradation*: Given a dense control tensor $D \in \mathbb{R}^{B \times C \times H \times W}$, we apply degradation with probability β using two techniques: *a) Random Scale Fusion*: A set of spatial scales $\{1, 1/2, \dots, 1/2^n\}$ is predefined. One scale is randomly excluded, and the remaining scales are used to generate downsampled versions of the input, which are then upsampled to the original resolution. Each version is assigned a random weight normalized to sum to 1. Their weighted sum forms a fused depth map with multi-scale degradation and randomness, enhancing robustness to spatial variation. *b) Adaptive Blur Augmentation*: An average blur with a randomly chosen odd-sized kernel is applied to the dense input to reduce sharpness, limiting the model’s tendency to overfit to local depth details.

Together, these degradations mitigate the model’s over-reliance on dense signals and enhance its ability to integrate complementary cues from sparse modalities, leading to more stable and consistent long-term video generation. During this pretraining stage, only the parameters of the control branches and fusion layers ϕ^l are updated, while the backbone remains frozen. This design introduces strong yet flexible conditioning from both dense and sparse modalities, preserving the stability and prior knowledge of the pre-trained base model.

2.2. Frame Degradation Training

The first image used in long-form video generation is itself a predicted frame whose quality gradually deteriorates over time, making it notably inferior to the clean images seen during training. As a result, the model tends to accumulate visual degradation across frames. Moreover, due to the non-lossless encoding and decoding process of the VAE, repeated reconstruction further amplifies this decline in quality.

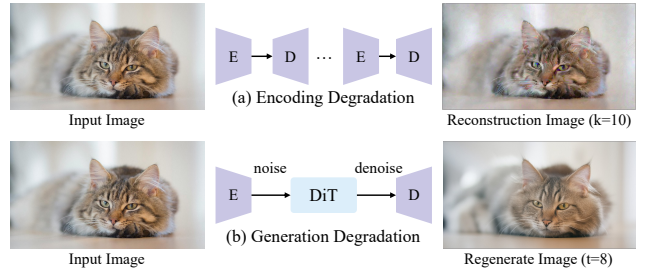


Figure 5. **Details of Frame Degradation.** We apply two types of degradation—VAE encoding and denoising—to simulate the quality decay that occurs during long-term generation.

To mitigate the gap between training and inference, we introduce a simple yet effective strategy: during training, we intentionally degrade the first image to mimic the corrupted inputs encountered in long-term generation. Specifically, we design two complementary degradation mechanisms that together define the degradation operator $\mathcal{T}(\cdot)$: **(1) Encoding degradation**: We simulate VAE-induced corruption by repeatedly encoding and decoding the first image K times through the VAE and storing the resulting degraded reconstructions. **(2) Generation degradation**: We simulate diffusion-based degradation by adding Gaussian noise to the latent representation of the first image at a random timestep t , followed by denoising through the diffusion model to obtain a restored version. Formally, the degradation process can be expressed as:

$$\mathcal{T}(I) = \begin{cases} (\mathcal{D} \circ \mathcal{E})^K(I), & w.p. 0.2, \\ \mathcal{D}(\Phi_0(\sqrt{\alpha_t}\mathcal{E}(I) + \sqrt{1 - \alpha_t}\epsilon)), & w.p. 0.8, \end{cases} \quad (4)$$

where I denotes the input image, $t < 15$, and $\epsilon \sim \mathcal{N}(0, \mathbf{I})$.

During training, we randomly apply $\mathcal{T}(\cdot)$ with a probability α , where the degradation severity is inversely proportional to its sampling probability—milder degradations occur more frequently, while stronger degradations are applied less often. This strategy effectively improves the visual quality of long video generation. However, despite the improved visual fidelity, this training scheme introduces a new issue of temporal inconsistency: the model tends to enhance



Figure 6. **Visual comparison across training stages.** The results indicate that the second stage alleviates visual degradation but introduces intra-clip inconsistency, which is subsequently resolved by the final stage of training.

the quality of the next clip independently, leading to noticeable discrepancies between adjacent clips. To mitigate this problem, we introduce the history-context guidance stage, which explicitly incorporates the preceding clip as contextual conditioning to enforce temporal coherence across clips.

2.3. History Context Guidance

To enhance temporal consistency between adjacent clips and further improve long-term coherence, we propose **History Context Guidance**. During training, we introduce history frames to encourage the model to learn causal temporal dependencies. Specifically, we first use the VAE encoder $\mathcal{E}(\cdot)$ to obtain the latent representations of the N_H history frames V_H , denoted as $z_H = \mathcal{E}(V_H)$. Following the masking mechanism in Wan, we apply an all-ones mask to the history latent z_H , forcing the model to reference historical context for maintaining temporal consistency. To align the training and long-term inference domains, we apply the degradation operator $\mathcal{T}(\cdot)$ to the history frames, producing degraded inputs $\tilde{V}_H = \mathcal{T}(V_H)$. The degraded frames are then encoded as: $\tilde{z}_H = \mathcal{E}(\tilde{V}_H)$. Our model can be formulated as:

$$z_t = \mathcal{F}(z_{t+1} | z_I, z_H, c_D, c_P), \quad (5)$$

where z_I denotes the latent representation of the initial frame, and c_D and c_P represent the dense and sparse control signals, respectively. Here, \mathcal{F} denotes the overall generative model.

In clip-based long video generation, the first frame of each clip serves as the temporal anchor linking consecutive segments. However, its latent representation may deviate from both the historical context and the degraded input, potentially weakening cross-clip coherence. To alleviate discontinuities at this boundary frame, we assign exponentially increasing weights $\{0.05, 0.325, 0.757\}$ to the latents of the first three generated frames, encouraging smoother early-frame transitions within each clip. In addition, we regularize the first latent of the predicted frames from complementary frequency perspectives to further stabilize this boundary frame. To jointly reinforce reconstruction fidelity and main-

tain smooth temporal boundaries, we introduce three loss terms as described below:

(1) History context consistency. We encourage the first predicted latent to align with the last latent of history context:

$$\mathcal{L}_{\text{cons}} = \|z_H^{-1} - \hat{z}^0\|^2, \quad (6)$$

where z_H^{-1} is the last latent of history segment and \hat{z}^0 is the first predicted latent.

(2) Degradation consistency. To maintain structural coherence with degraded inputs and stabilize clip boundaries, we impose low-frequency consistency:

$$\mathcal{L}_{\text{deg}} = \|\mathcal{F}_{\text{lp}}(\tilde{z}_I^0) - \mathcal{F}_{\text{lp}}(\hat{z}^0)\|^2, \quad (7)$$

where \tilde{z}_I^0 is the latent of the degraded first image and $\mathcal{F}_{\text{lp}}(\cdot)$ denotes a low-frequency extraction operator.

(3) Ground-truth high-frequency alignment. To preserve fine-grained appearance details, we align high-frequency components with the ground truth:

$$\mathcal{L}_{\text{gt}} = \|\mathcal{F}_{\text{hp}}(z_{\text{gt}}^0) - \mathcal{F}_{\text{hp}}(\hat{z}^0)\|^2, \quad (8)$$

where $\mathcal{F}_{\text{hp}}(\cdot)$ denotes a high-frequency operator.

The final temporal regularization objective is defined as:

$$\mathcal{L}_{\text{temp}} = \lambda_{\text{deg}}\mathcal{L}_{\text{deg}} + \lambda_{\text{gt}}\mathcal{L}_{\text{gt}} + \lambda_{\text{cons}}\mathcal{L}_{\text{cons}}. \quad (9)$$

In practice, we set $\lambda_{\text{deg}} = 0.2$, $\lambda_{\text{gt}} = 0.15$ and $\lambda_{\text{cons}} = 0.5$. To further capture the causal dependencies of historical information, we additionally update all parameters in the self-attention layers of the base model. The number of history frames N_H is uniformly sampled from $[0, 16]$, enabling LongVie 2 to perform unified long-video inference—whether or not historical references are available. This contextual conditioning substantially enhances temporal continuity and cross-clip consistency, resulting in smoother and more coherent long-video generation.

2.4. Training-free Inter-clip Consistency Strategies

To further improve temporal coherence across adjacent clips, we introduce two complementary **training-free** strategies that enhance inter-clip consistency.

Unified Noise Initialization. To further enhance temporal stability and consistency during video generation, we adopt a unified noise initialization across all video clips. Rather than sampling a new noise latent for each clip, a single shared noise instance is maintained throughout the entire sequence, providing a coherent stochastic prior that strengthens temporal continuity and overall coherence.

Global Normalization. Independent normalization of control inputs across clips often causes temporal discontinuities, as each segment may adopt a different depth scale. To mitigate this, we employ a global normalization strategy applied to the entire depth sequence. Specifically, we compute the 5th and 95th percentiles of all pixel values across the full video and use them as the global minimum and maximum bounds. The depth values are then clipped to this range and linearly scaled to $[0, 1]$. This percentile-based normalization is robust to outliers and ensures a consistent depth scale across clips. After normalization, the depth sequence is divided into overlapping clips to match the autoregressive inference process and enable point-map extraction.

3. Experiments

Implementation Details. The video diffusion backbone of LongVie 2 is Wan2.1-I2V-14B [40]. We replicate the first 12 DiT blocks to construct a dedicated control branch and further split each copied block along the feature dimension to form dense and sparse control pathways, effectively reducing computational overhead. During training, we first extract depth maps using Video Depth Anything [7] as dense control signals, and then apply SpatialTracker [41] to estimate and track 3D points from the normalized depth. Following DAS [13], we uniformly sample 4,900 points per clip as sparse control inputs. In total, around 100000 videos are used for training. In the first and second stages, approximately 60000 videos from ACID [26], Vchitect-T2V-DataVerse [11], and MovieNet [21] are employed. Each video is divided into 81-frame clips with a resolution of 352×640 at 16 fps to save memory and improve efficiency. LongVie 2 is optimized with AdamW at a learning rate of 1×10^{-5} , updating only the control branch parameters. In the final stage, longer videos are incorporated to enable temporal reasoning over extended sequences. About 40000 videos from OmniWorld [57] and SpatialVID [38] are used, all downsampled to 352×640 at 16 fps. This stage employs AdamW with a learning rate of 5×10^{-6} and updates the parameters in both the self-attention layers and the control modules. All three stages are conducted on 16 A100 GPUs with each GPU using a batch size of 1, for approximately

5000, 1000, and 2000 iterations, respectively. The full training process takes about two days.

LongVGenBench. To address the absence of suitable benchmarks for controllable long video generation, we introduce LongVGenBench—a dataset of 100 one-shot videos, each exceeding one minute in duration at 1080p resolution. Existing datasets fall short in this regard, as they lack long, continuous, one-shot videos that are essential for evaluating temporal consistency and controllability. LongVGenBench covers diverse real-world and game-based scenarios and includes challenging cases such as rapid scene transitions and complex object motions (see the supplementary material for details), establishing it as a comprehensive and demanding benchmark for long video generation. For evaluation, each video is divided into 81-frame clips at 16 fps with a one-frame overlap, following the autoregressive setup used in our experiments. Captions are automatically generated by Qwen2.5-VL-7B [1] to serve as text prompts, and corresponding control signals are extracted from each clip. During validation, the first frame of each video is left unaltered to ensure fair comparison and to enable accurate assessment of generation quality against ground-truth references.

3.1. Qualitative Comparison

To comprehensively and fairly evaluate the performance of LongVie 2, we employ both objective and subjective metrics for comparison with existing baselines.

Objective Evaluation. We first evaluate the effectiveness of LongVie 2 by comparing it against three categories of baselines: (1) *Pretrained video models*: Wan2.1 [43]; (2) *Controllable models*: VideoComposer [39], Go-with-the-Flow [3], DAS [13], and Motion-I2V [34]; (3) *World models*: Hunyuan-GameCraft [24] and Matrix-Game [16]. Following the widely adopted VBench protocol [23], we evaluate performance using seven metrics—*Background Consistency (B.C.)*, *Subject Consistency (S.C.)*, *Overall Consistency (Q.C.)*, *Dynamic Degree (D.D.)*, *Aesthetic Quality (A.Q.)*, and *Imaging Quality (I.Q.)*—to assess temporal coherence and visual fidelity. We also report similarity-based metrics, including SSIM and LPIPS, to measure the controllability of the generated videos.

As shown in Tab. 1, LongVie 2 achieves substantial improvements over controllable baselines in controllability, and surpasses existing other baselines in both temporal consistency and visual quality. These results demonstrate that LongVie 2 effectively maintains high controllability while producing long videos of superior visual coherence and quality, achieving state-of-the-art performance.

Human Evaluation. To further assess the perceptual quality of long video generation, we conduct a carefully designed human evaluation study. To mitigate participant fatigue, the study follows a balanced and randomized sampling protocol. From all generated videos, we randomly select 80 samples,

Table 1. **Quantitative comparison of LongVie 2 and baselines on LongVGenBench.** We compare **LongVie 2** with base diffusion models, controllable generation models, and world models on **LongVGenBench**, evaluating *visual quality*, *controllability*, and *long-term consistency*. **Bold** indicates the best performance, and underline denotes the second-best.

METHODS	Quality		Controllability		Temporal Consistency			
	A.Q.↑	I.Q.↑	SSIM↑	LPIPS↓	S.C.↑	B.C.↑	O.C.↑	D.D.↑
Wan2.1 [40]	49.72%	63.78%	0.406	0.488	83.56%	88.86%	20.30%	15.15%
VideoComposer [39]	43.53%	59.33%	0.346	0.583	80.33%	88.30%	19.83%	27.78%
Motion-I2V [34]	48.34%	61.57%	0.385	0.504	82.35%	89.25%	20.46%	44.13%
Go-With-The-Flow [3]	53.59%	62.21%	0.453	0.394	84.37%	90.62%	<u>21.79%</u>	46.15%
DiffusionAsShader [13]	53.28%	64.57%	0.401	0.482	<u>86.06%</u>	<u>90.78%</u>	21.10%	36.76%
Matrix-Game-2.0 [16]	55.24%	59.23%	0.427	0.501	77.82%	76.43%	19.37%	74.45%
HunyuanGameCraft [24]	<u>56.18%</u>	<u>67.73%</u>	<u>0.483</u>	<u>0.386</u>	79.12%	74.24%	20.94%	<u>80.46%</u>
LongVie 2 (Ours)	58.47%	69.77%	0.529	0.295	91.05%	92.45%	23.37%	82.95%



Figure 7. **Controllability comparison between LongVie 2 and baselines.** LongVie 2 demonstrates markedly superior controllability, maintaining precise structural alignment and realistic appearance across frames compared with the baselines. *GWF* denotes *Go-With-The-Flow*, and *DAS* denotes *Diffusion as Shader*.

Table 2. **Human Evaluation Results.** Sixty participants rated LongVie 2 and baseline models across five evaluation dimensions. LongVie 2 consistently achieved the highest scores in all aspects.

METHOD	VQ	PVC	CC	CoIC	TC
Matrix-Game-2.0 [16]	2.12	2.08	2.27	2.23	2.37
Go-With-The-Flow [3]	2.34	2.32	2.18	2.26	2.02
DiffusionAsShader [13]	3.03	3.07	3.09	3.02	2.79
HunyuanGameCraft [24]	3.11	3.14	3.28	3.37	3.35
LongVie (Ours)	4.40	4.39	4.18	4.12	4.53

each paired with its corresponding prompt and control signals. Participants evaluate five key aspects: *Visual Quality (VQ)*, *Prompt–Video Consistency (PVC)*, *Condition Consistency (CC)*, *Color Consistency (CoIC)*, and *Temporal Consistency (TC)*. We compare five representative models—Go-With-The-Flow [3], DAS [13], HunyuanGameCraft [24], Matrix-Game [16], and LongVie 2. A total of 60 participants are recruited. For each evaluation aspect, they rank the models from best to worst, assigning scores from 5 to 1 accordingly. The averaged results, summarized in Tab. 2, show that LongVie 2 consistently attains the highest scores across all criteria, demonstrating its superior perceptual quality and

controllability.

3.2. Quantitative Results

To comprehensively demonstrate the performance of LongVie 2, we present results from two key aspects: *controllability* and *long-term quality & consistency*.

Controllability Comparison. To verify that LongVie 2 preserves controllability, we directly evaluate it on standard controllable video generation tasks and compare it with strong baselines, including DAS [13] and GWF [3]. As illustrated in Fig. 7, our model consistently outperforms the baselines across three representative sub-tasks: motion transfer, style transfer, and mesh-to-video generation. It can be observed that LongVie 2 achieves superior controllability and produces finer visual details under the same settings.

Long-Term Generation Results. We further present long-duration generation results of LongVie 2 in Fig. 8. Each row depicts a video exceeding two minutes in length, demonstrating the model’s ability to maintain high visual fidelity and long-term temporal coherence. Notably, under world-level guidance, the model can simulate realistic physical phenomena such as the flow change after turning a faucet



Figure 8. **Long-term generation demos.** We present several videos generated by **LongVie 2**, each lasting over two minutes, demonstrating sustained visual quality and long-term temporal consistency, further validating the effectiveness of our training strategy.

Table 3. **Ablation on staged training of LongVie 2.** We progressively introduce three stages: *Control Learning*, *Degradation Adaptation*, and *History Context*. Each stage consistently enhances visual quality, controllability, and long-term consistency.

TRAINING STRATEGY	Quality		Controllability		Temporal Consistency			
	A.Q.↑	I.Q.↑	SSIM↑	LPIPS↓	S.C.↑	B.C.↑	O.C.↑	D.D.↑
Base Model	49.72%	63.78%	0.406	0.488	83.56%	88.86%	20.30%	15.15%
+ Control Learning	51.36%	64.32%	0.456	0.376	85.94%	90.42%	20.95%	73.62%
+ Degradation Adaptation	54.08%	66.21%	0.501	0.328	88.12%	91.05%	21.56%	76.12%
+ History Context	58.47%	69.77%	0.529	0.295	91.05%	92.45%	23.37%	82.59%

Table 4. **Ablation study for our proposed components.** The █ block denotes experiments targeting temporal consistency, while the █ block denotes those focusing on visual quality.

METHODS	A.Q.	I.Q.	S.C.	B.C.
Full model	58.47%	69.77%	91.05%	92.45%
w/o Global Normalization	57.73%	69.56%	88.81%	91.41%
w/o Unified Initial Noise	57.80%	69.62%	88.73%	91.59%
w/o Both	57.03%	68.89%	88.56%	91.37%
w/o Feature Degradation	56.92%	67.23%	89.94%	92.15%
w/o Data Degradation	57.11%	67.84%	89.71%	92.08%
w/o Both	56.74%	67.01%	89.57%	91.99%

on or off, highlighting its capability for world-consistent video synthesis and further demonstrating the effectiveness of LongVie 2. Additional long-form results are provided in the supplementary material for a more comprehensive evaluation.

3.3. Ablation Study

We conduct ablation studies to verify the effectiveness of each component and training strategy adopted in our method. **Stage-Wise Training.** LongVie 2 is trained in three progressive stages, each designed to enhance different aspects of video generation. To examine the contribution of each stage, we systematically remove them and report the results in Tab. 3. The first stage yields a clear improvement in SSIM and LPIPS, indicating stronger controllability. The second

stage further enhances visual quality through degradation-aware learning, while the third stage notably improves global temporal consistency by incorporating history-context guidance. These results confirm that our stage-wise training strategy is both necessary and effective.

Unified Initial Noise & Global Normalization. We further analyze the influence of unified initial noise and global normalization of control signals on temporal stability and controllability. Videos are generated under three configurations: (1) without Global Normalization, (2) without Unified Initial Noise, and (3) without both. As shown in Tab. 4, removing either component leads to performance drops across all metrics, indicating that unified noise initialization and global normalization are both beneficial for consistent and high-quality controllable long video generation.

4. Related Works

Controllable Video Generation. Recent advances in controllable video generation have enabled the synthesis of visually compelling and semantically aligned videos under diverse structural and motion constraints. VideoComposer [39] enhances controllability through multiple conditioning signals. Following the ControlNet [52] paradigm, SparseCtrl [14] introduces sparse structural guidance for fine-grained control, while Go-With-The-Flow [3] and MotionI2V [34] utilize optical flow to direct temporal motion. DAS [13] further employs 3D point maps for precise spatial and motion control. More recently, Cosmos-Transfer-1 [30] and LongVie [12] integrate multi-modal control signals to jointly

improve visual fidelity and alignment in controllable video synthesis.

World Models. Recent advances in video world modeling are powered by large-scale transformer and diffusion architectures that generate high-fidelity, temporally coherent videos conditioned on actions or camera trajectories. A series of world models [2, 8, 16, 19, 24, 29, 44, 50, 53, 58] follow this paradigm, focusing on camera-control-based simulation of dynamic environments. Leveraging large-scale video or gameplay data, these systems learn controllable and physically plausible dynamics, marking an important step toward general-purpose video world models capable of synthesizing consistent and interactive scenes under explicit control.

Long Video Generation. Generating long, coherent videos remains a fundamental challenge due to accumulated temporal drift and quality degradation over extended horizons. StreamingT2V [17] adopts an autoregressive strategy to progressively extend video length. Diffusion Forcing [6, 35, 49] introduces causal constraints to improve temporal stability, while TTT [10], LCT [15], and MoC [4] explicitly incorporate long-range contextual dependencies to enhance visual and temporal consistency. More recently, SVI [25] proposes an error-recycling fine-tuning paradigm that exposes the model to its own autoregressive outputs, thereby mitigating the mismatch between short-clip training and long-form inference. In parallel, Self-Forcing [22] leverages video-level distribution-matching objectives [47, 48], together with related extensions [9, 27, 28, 42, 45, 46, 51, 54, 59], to achieve long-horizon stability through autoregressive rollout and self-consistent training. Inspired by the growing emphasis on narrowing the train-test discrepancy, we introduce a simple yet effective approach that simulates long-form degradation directly on the input frames during training, enabling the model to better preserve visual fidelity and temporal coherence over extended durations.

5. Conclusion

In this work, we explore how to extend pretrained video diffusion models toward building general-purpose video world models capable of generating coherent, controllable, and temporally consistent long videos. We empirically demonstrate that strengthening controllability before enhancing long-term visual quality is an effective and practical strategy, and we propose **LongVie 2**, a three-stage autoregressive framework that progressively improves controllability, visual fidelity, and long-term consistency. First, we integrate dense and sparse controls to inject world-level guidance, providing complementary structural and semantic cues. Second, a degradation-aware training strategy applied to first-frame inputs bridges the gap between training and long-horizon inference. Finally, history context guidance models long-range dependencies to maintain temporal coherence across

extended sequences. To enable comprehensive evaluation, we establish **LongVGenBench**, a benchmark containing 100 one-minute videos covering diverse real-world and synthetic environments. Extensive experiments demonstrate that LongVie 2 achieves state-of-the-art performance in controllable long video generation and can autoregressively synthesize high-quality videos lasting up to 3–5 minutes, marking a significant step toward video world modeling.

References

- [1] Shuai Bai, Keqin Chen, Xuejing Liu, Jialin Wang, Wenbin Ge, Sibo Song, Kai Dang, Peng Wang, Shijie Wang, Jun Tang, Humen Zhong, Yuanzhi Zhu, Mingkun Yang, Zhaohai Li, Jianqiang Wan, Pengfei Wang, Wei Ding, Zheren Fu, Yiheng Xu, Jiabo Ye, Xi Zhang, Tianbao Xie, Zesen Cheng, Hang Zhang, Zhibo Yang, Haiyang Xu, and Junyang Lin. Qwen2.5-vl technical report. *arXiv preprint arXiv:2502.13923*, 2025. 6, 1
- [2] Philip J. Ball et al. Genie 3: A new frontier for world models. 2025. 9
- [3] Ryan Burgert, Yuancheng Xu, Wenqi Xian, Oliver Pilarski, Pascal Clausen, Mingming He, Li Ma, Yitong Deng, Lingxiao Li, Mohsen Mousavi, Michael Ryoo, Paul Debevec, and Ning Yu. Go-with-the-flow: Motion-controllable video diffusion models using real-time warped noise. In *CVPR*, 2025. Licensed under Modified Apache 2.0 with special crediting requirement. 6, 7, 8
- [4] Shengqu Cai, Ceyuan Yang, Lvmin Zhang, Yuwei Guo, Junfei Xiao, Ziyang Yang, Yinghao Xu, Zhenheng Yang, Alan Yuille, Leonidas Guibas, et al. Mixture of contexts for long video generation. *arXiv preprint arXiv:2508.21058*, 2025. 9
- [5] Brandon Castellano. Pyscenedetect. <https://github.com/Breakthrough/PySceneDetect>, 2024. Video Cut Detection and Analysis Tool. Available at <https://www.scenedetect.com>. Accessed: 2025-05-19. 1
- [6] Boyuan Chen, Diego Martí Monsó, Yilun Du, Max Simchowitz, Russ Tedrake, and Vincent Sitzmann. Diffusion forcing: Next-token prediction meets full-sequence diffusion. *Advances in Neural Information Processing Systems*, 37:24081–24125, 2024. 9
- [7] Sili Chen, Hengkai Guo, Shengnan Zhu, Feihu Zhang, Zilong Huang, Jiashi Feng, and Bingyi Kang. Video depth anything: Consistent depth estimation for super-long videos. *arXiv:2501.12375*, 2025. 6, 1
- [8] Taiye Chen, Xun Hu, Zihan Ding, and Chi Jin. Learning world models for interactive video generation. *arXiv preprint arXiv:2505.21996*, 2025. 9
- [9] Justin Cui, Jie Wu, Ming Li, Tao Yang, Xiaojie Li, Rui Wang, Andrew Bai, Yuanhao Ban, and Cho-Jui Hsieh. Self-forcing++: Towards minute-scale high-quality video generation. *arXiv preprint arXiv:2510.02283*, 2025. 9
- [10] Karan Dalal, Daniel Kocreja, Gashon Hussein, Jiarui Xu, Yue Zhao, Youjin Song, Shihao Han, Ka Chun Cheung, Jan Kautz, Carlos Guestrin, Tatsunori Hashimoto, Sanmi Koyejo, Yejin Choi, Yu Sun, and Xiaolong Wang. One-minute video generation with test-time training, 2025. 9

- [11] Weichen Fan, Chenyang Si, Junhao Song, Zhenyu Yang, Yanan He, Long Zhuo, Ziqi Huang, Ziyue Dong, Jingwen He, Dongwei Pan, et al. Vchitect-2.0: Parallel transformer for scaling up video diffusion models. *arXiv preprint arXiv:2501.08453*, 2025. 1, 6
- [12] Jianxiong Gao, Zhaoxi Chen, Xian Liu, Jianfeng Feng, Chenyang Si, Yanwei Fu, Yu Qiao, and Ziwei Liu. Longvie: Multimodal-guided controllable ultra-long video generation, 2025. 8
- [13] Zekai Gu, Rui Yan, Jiahao Lu, Peng Li, Zhiyang Dou, Chenyang Si, Zhen Dong, Qifeng Liu, Cheng Lin, Ziwei Liu, Wenping Wang, and Yuan Liu. Diffusion as shader: 3d-aware video diffusion for versatile video generation control. *arXiv preprint arXiv:2501.03847*, 2025. 3, 6, 7, 8
- [14] Yuwei Guo, Ceyuan Yang, Anyi Rao, Maneesh Agrawala, Dahua Lin, and Bo Dai. Sparsectrl: Adding sparse controls to text-to-video diffusion models. In *European Conference on Computer Vision*, pages 330–348. Springer, 2024. 8
- [15] Yuwei Guo, Ceyuan Yang, Ziyang Yang, Zhibei Ma, Zhijie Lin, Zhenheng Yang, Dahua Lin, and Lu Jiang. Long context tuning for video generation, 2025. 9
- [16] Xianglong He, Chunli Peng, Zexiang Liu, Boyang Wang, Yifan Zhang, Qi Cui, Fei Kang, Biao Jiang, Mengyin An, Yangyang Ren, Baixin Xu, Hao-Xiang Guo, Kaixiong Gong, Cyrus Wu, Wei Li, Xuchen Song, Yang Liu, Eric Li, and Yahui Zhou. Matrix-game 2.0: An open-source, real-time, and streaming interactive world model. *arXiv preprint arXiv:2508.13009*, 2025. 2, 6, 7, 9
- [17] Roberto Henschel, Levon Khachatryan, Hayk Poghosyan, Daniil Hayrapetyan, Vahram Tadevosyan, Zhangyang Wang, Shant Navasardyan, and Humphrey Shi. Streamingt2v: Consistent, dynamic, and extendable long video generation from text, 2025. 9
- [18] Jonathan Ho, Ajay Jain, and Pieter Abbeel. Denoising diffusion probabilistic models, 2020. 1
- [19] Yicong Hong, Yiqun Mei, Chongjian Ge, Yiran Xu, Yang Zhou, Sai Bi, Yannick Hold-Geoffroy, Mike Roberts, Matthew Fisher, Eli Shechtman, et al. Relic: Interactive video world model with long-horizon memory. *arXiv preprint arXiv:2512.04040*, 2025. 9
- [20] Edward J. Hu, Yelong Shen, Phillip Wallis, Zeyuan Allen-Zhu, Yuanzhi Li, Shean Wang, Lu Wang, and Weizhu Chen. Lora: Low-rank adaptation of large language models, 2021. 2
- [21] Qingqiu Huang, Yu Xiong, Anyi Rao, Jiaze Wang, and Dahua Lin. Movienet: A holistic dataset for movie understanding. In *Computer Vision—ECCV 2020: 16th European Conference, Glasgow, UK, August 23–28, 2020, Proceedings, Part IV 16*, pages 709–727. Springer, 2020. 6, 1
- [22] Xun Huang, Zhengqi Li, Guande He, Mingyuan Zhou, and Eli Shechtman. Self forcing: Bridging the train-test gap in autoregressive video diffusion. *arXiv preprint arXiv:2506.08009*, 2025. 9
- [23] Ziqi Huang, Yanan He, Jiashuo Yu, Fan Zhang, Chenyang Si, Yuming Jiang, Yuanhan Zhang, Tianxing Wu, Qingyang Jin, Nattapol Chanpaisit, Yaohui Wang, Xinyuan Chen, Limin Wang, Dahua Lin, Yu Qiao, and Ziwei Liu. VBench: Comprehensive benchmark suite for video generative models. In *Proceedings of the IEEE/CVF Conference on Computer Vision and Pattern Recognition*, 2024. 6
- [24] Jiaqi Li, Junshu Tang, Zhiyong Xu, Longhuang Wu, Yuan Zhou, Shuai Shao, Tianbao Yu, Zhiguo Cao, and Qinglin Lu. Hunyuan-gamecraft: High-dynamic interactive game video generation with hybrid history condition, 2025. 2, 6, 7, 9
- [25] Wuyang Li, Wentao Pan, Po-Chien Luan, Yang Gao, and Alexandre Alahi. Stable video infinity: Infinite-length video generation with error recycling. *arXiv preprint arXiv:2510.09212*, 2025. 9
- [26] Andrew Liu, Richard Tucker, Varun Jampani, Ameesh Makadia, Noah Snavely, and Angjoo Kanazawa. Infinite nature: Perpetual view generation of natural scenes from a single image. In *Proceedings of the IEEE/CVF International Conference on Computer Vision (ICCV)*, 2021. 6, 1
- [27] Kunhao Liu, Wenbo Hu, Jiale Xu, Ying Shan, and Shijian Lu. Rolling forcing: Autoregressive long video diffusion in real time. *arXiv preprint arXiv:2509.25161*, 2025. 9
- [28] Yunhong Lu, Yanhong Zeng, Haobo Li, Hao Ouyang, Qiyu Wang, Ka Leong Cheng, Jiapeng Zhu, Hengyuan Cao, Zhipeng Zhang, Xing Zhu, et al. Reward forcing: Efficient streaming video generation with rewarded distribution matching distillation. *arXiv preprint arXiv:2512.04678*, 2025. 9
- [29] Xiaofeng Mao, Shaoheng Lin, Zhen Li, Chuanhao Li, Wenshuo Peng, Tong He, Jiangmiao Pang, Mingmin Chi, Yu Qiao, and Kaipeng Zhang. Yume: An interactive world generation model. *arXiv preprint arXiv:2507.17744*, 2025. 2, 9
- [30] NVIDIA. Cosmos-transfer1: Conditional world generation with adaptive multimodal control, 2025. 8
- [31] OpenAI. Sora. Accessed February 15, 2024 [Online] <https://sora.com/library>, 2024. 1
- [32] Adam Polyak, Amit Zohar, et al. Movie gen: A cast of media foundation models, 2025. 1
- [33] Robin Rombach, Andreas Blattmann, Dominik Lorenz, Patrick Esser, and Björn Ommer. High-resolution image synthesis with latent diffusion models, 2021. 1, 3
- [34] Xiaoyu Shi, Zhaoyang Huang, Fu-Yun Wang, Weikang Bian, Dasong Li, Yi Zhang, Manyuan Zhang, Ka Chun Cheung, Simon See, Hongwei Qin, et al. Motion-i2v: Consistent and controllable image-to-video generation with explicit motion modeling. In *ACM SIGGRAPH 2024 Conference Papers*, pages 1–11, 2024. 6, 7, 8
- [35] Kiwhan Song, Boyuan Chen, Max Simchowitz, Yilun Du, Russ Tedrake, and Vincent Sitzmann. History-guided video diffusion, 2025. 9
- [36] Hunyuan Foundation Model Team. Hunyuanvideo: A systematic framework for large video generative models, 2024. 1
- [37] Kuaishou Team. Kling. Accessed December 9, 2024 [Online] <https://klingai.kuaishou.com/>, 2024. 1
- [38] Jiahao Wang, Yufeng Yuan, Rujie Zheng, Youtian Lin, Jian Gao, Lin-Zhuo Chen, Yajie Bao, Yi Zhang, Chang Zeng, Yanxi Zhou, et al. Spatialvid: A large-scale video dataset with spatial annotations. *arXiv preprint arXiv:2509.09676*, 2025. 6, 1
- [39] Xiang Wang, Hangjie Yuan, Shiwei Zhang, Dayou Chen, Jiuniu Wang, Yingya Zhang, Yujun Shen, Deli Zhao, and Jingren Zhou. Videocomposer: Compositional video synthesis

- with motion controllability. *Advances in Neural Information Processing Systems*, 36:7594–7611, 2023. 6, 7, 8
- [40] WanTeam. Wan: Open and advanced large-scale video generative models. *arXiv preprint arXiv:2503.20314*, 2025. 1, 6, 7, 2
- [41] Yuxi Xiao, Qianqian Wang, Shangzhan Zhang, Nan Xue, Sida Peng, Yujun Shen, and Xiaowei Zhou. Spatialtracker: Tracking any 2d pixels in 3d space. In *Proceedings of the IEEE/CVF Conference on Computer Vision and Pattern Recognition (CVPR)*, 2024. 6, 1
- [42] Shuai Yang, Wei Huang, Ruihang Chu, Yicheng Xiao, Yuyang Zhao, Xianbang Wang, Muyang Li, Enze Xie, Yingcong Chen, Yao Lu, Song Han, and Yukang Chen. Longlive: Real-time interactive long video generation, 2025. 9
- [43] Zhuoyi Yang, Jiayan Teng, Wendi Zheng, Ming Ding, Shiyu Huang, Jiazheng Xu, Yuanming Yang, Wenyi Hong, Xiaohan Zhang, Guanyu Feng, et al. Cogvideox: Text-to-video diffusion models with an expert transformer. *arXiv preprint arXiv:2408.06072*, 2024. 1, 6
- [44] Deheng Ye, Fangyun Zhou, Jiacheng Lv, Jianqi Ma, Jun Zhang, Junyan Lv, Junyou Li, Minwen Deng, Mingyu Yang, Qiang Fu, Wei Yang, Wenkai Lv, Yangbin Yu, Yewen Wang, Yonghang Guan, Zhihao Hu, Zhongbin Fang, and Zhongqian Sun. Yan: Foundational interactive video generation, 2025. 9
- [45] Hidir Yesiltepe, Tuna Han Salih Meral, Adil Kaan Akan, Kaan Oktay, and Pinar Yanardag. Infinity-rope: Action-controllable infinite video generation emerges from autoregressive self-rollback. *arXiv preprint arXiv:2511.20649*, 2025. 9
- [46] Jung Yi, Wooseok Jang, Paul Hyunbin Cho, Jisu Nam, Heeji Yoon, and Seungryong Kim. Deep forcing: Training-free long video generation with deep sink and participative compression. *arXiv preprint arXiv:2512.05081*, 2025. 9
- [47] Tianwei Yin, Michaël Gharbi, Taesung Park, Richard Zhang, Eli Shechtman, Fredo Durand, and William T Freeman. Improved distribution matching distillation for fast image synthesis. In *NeurIPS*, 2024. 9
- [48] Tianwei Yin, Michaël Gharbi, Richard Zhang, Eli Shechtman, Frédo Durand, William T Freeman, and Taesung Park. One-step diffusion with distribution matching distillation. In *CVPR*, 2024. 9
- [49] Tianwei Yin, Qiang Zhang, Richard Zhang, William T Freeman, Fredo Durand, Eli Shechtman, and Xun Huang. From slow bidirectional to fast autoregressive video diffusion models. In *CVPR*, 2025. 9
- [50] Jiwen Yu, Yiran Qin, Xintao Wang, Pengfei Wan, Di Zhang, and Xihui Liu. Gamefactory: Creating new games with generative interactive videos, 2025. 9
- [51] Yifei Yu, Xiaoshan Wu, Xinting Hu, Tao Hu, Yangtian Sun, Xiaoyang Lyu, Bo Wang, Lin Ma, Yuewen Ma, Zhongrui Wang, et al. Videossm: Autoregressive long video generation with hybrid state-space memory. *arXiv preprint arXiv:2512.04519*, 2025. 9
- [52] Lvmin Zhang, Anyi Rao, and Maneesh Agrawala. Adding conditional control to text-to-image diffusion models, 2023. 2, 3, 8
- [53] Yifan Zhang, Chunli Peng, Boyang Wang, Puyi Wang, Qingcheng Zhu, Fei Kang, Biao Jiang, Zedong Gao, Eric Li, Yang Liu, et al. Matrix-game: Interactive world foundation model. *arXiv preprint arXiv:2506.18701*, 2025. 9
- [54] Zeyu Zhang, Shuning Chang, Yuanyu He, Yizeng Han, Jiasheng Tang, Fan Wang, and Bohan Zhuang. Blockvid: Block diffusion for high-quality and consistent minute-long video generation, 2025. 9
- [55] Zangwei Zheng, Xiangyu Peng, Tianji Yang, Chenhui Shen, Shenggui Li, Hongxin Liu, Yukun Zhou, Tianyi Li, and Yang You. Open-sora: Democratizing efficient video production for all. *arXiv preprint arXiv:2412.20404*, 2024. 1
- [56] Tinghui Zhou, Richard Tucker, John Flynn, Graham Fyffe, and Noah Snavely. Stereo magnification: Learning view synthesis using multiplane images. *ACM Trans. Graph. (Proc. SIGGRAPH)*, 37, 2018. 1
- [57] Yang Zhou, Yifan Wang, Jianjun Zhou, Wenzheng Chang, Haoyu Guo, Zizun Li, Kaijing Ma, Xinyue Li, Yating Wang, Haoyi Zhu, et al. Omniworld: A multi-domain and multi-modal dataset for 4d world modeling. *arXiv preprint arXiv:2509.12201*, 2025. 6, 1
- [58] Yixuan Zhu, Jiaqi Feng, Wenzhao Zheng, Yuan Gao, Xin Tao, Pengfei Wan, Jie Zhou, and Jiwen Lu. Astra: General interactive world model with autoregressive denoising, 2025. 9
- [59] Junhao Zhuang, Shi Guo, Xin Cai, Xiaohui Li, Yihao Liu, Chun Yuan, and Tianfan Xue. Flashvsr: Towards real-time diffusion-based streaming video super-resolution. *arXiv preprint arXiv:2510.12747*, 2025. 9

LongVie 2: Multimodal Controllable Ultra-Long Video World Model

Supplementary Material

6. Overview of Supplementary Material

This supplementary document provides additional technical details, datasets, and qualitative analyses to complement the main paper. In Sec. 7, we elaborate on the implementation details of **LongVie**, including the training data, inference adaptation strategy, and model configuration. In Sec. 8, we offer a comprehensive description of the **LongVGenBench** dataset used for evaluating long-term consistency and controllability. In Sec. 9, we conduct ablation studies on the key components of our frame degradation training strategy. In Sec. 10, we provide additional qualitative results under diverse styles and scenarios, including ultra-long video cases.

7. More Implementation Details

7.1. Training Data

Data for Stage 1 & Stage 2. As described in the *Implementation Details* section of the main paper, Stages 1 and 2 are trained on approximately 60,000 videos sourced from three complementary datasets. (1) *ACID and ACID-Large* [26] provide thousands of aerial drone videos capturing diverse coastlines, natural landscapes, and outdoor environments. The videos follow the same format as *RealEstate10K* [56], ensuring consistent metadata and camera-trajectory structure. (2) *Vchitect_T2V_DataVerse* [11] is a large-scale corpus of more than 14 million high-quality Internet videos, each paired with descriptive and fine-grained textual annotations, offering rich appearance and motion diversity for training. (3) *MovieNet* [21] contains 1,100 full-length movies spanning multiple decades, regions, and genres, providing complex scenes, camera motions, and human-centric activities. To standardize temporal resolution and facilitate stable training, all videos from these sources are uniformly converted into 81-frame clips sampled at 16 fps.

Data for Stage 3. Stage 3 focuses on long-horizon temporal modeling and therefore requires explicit history context inputs. To support this stage, we incorporate long-form videos from *OmniWorld* [57] and *SpatialVID* [38], which contain extended sequences with coherent scene dynamics. For each video, we extract 81-frame target segments beginning from the 20th frame; these segments serve as the prediction targets for the model. The corresponding control signals and textual prompts are generated following the same pipeline as Stages 1 and 2. During training, all frames preceding each 81-frame segment are loaded as the history context, enabling the model to learn long-range dependencies and temporal evolution. From the complete set of processed samples, we randomly select 40,000 segments to construct the Stage 3

training split.

Data Pre-processing. During our experiments, we observed that the presence of scene transitions (*e.g.* cuts or abrupt changes in viewpoint) in the training data can significantly undermine temporal consistency during long-horizon generation, often leading to undesired transitions in the synthesized videos. To alleviate this issue, we apply the *PySceneDetect* toolkit [5] to automatically identify scene boundaries and segment each raw video into transition-free clips. Each resulting segment is uniformly sampled at 16 fps and truncated to 81 consecutive frames to form a stable and temporally coherent training unit for *LongVie*. For each 81-frame clip, we compute a comprehensive set of control signals. Depth maps are extracted using *Video Depth Anything* [7], and point trajectories are estimated with *SpatialTracker* [41], leveraging both the depth information and RGB frames. In addition, we generate descriptive captions for every clip using *Qwen-2.5-VL-7B* [1] to provide semantically rich and contextually aligned textual guidance. After applying this unified pre-processing pipeline to all videos, we obtain a curated corpus of approximately 100,000 video-control signal pairs. This dataset serves as the complete training foundation for *LongVie*, enabling consistent learning across diverse visual domains and motion patterns.

7.2. Inference Preparation.

Point tracking naturally degrades during long-horizon inference because the tracked points depend on content visible in the first frame. As the video evolves—particularly when the originally tracked objects move out of view—the sparse tracks become unreliable. In our framework, point tracking acts as a sparse motion-control signal rather than an appearance cue. To preserve its effectiveness, we do not compute point tracks directly over the entire minute-long video. Instead, we first extract depth maps for the full sequence and apply global normalization across the entire duration. The video is then partitioned into overlapping 81-frame clips, and colorful point tracks are computed independently for each clip using the globally normalized depth, ensuring stable and consistent motion guidance throughout the generation process. A similar challenge arises with captions. In transfer scenarios, the original captions of the source videos often become semantically misaligned with the visual content after transformation. To address this mismatch and remain consistent with our training pipeline, we apply *Qwen-2.5-VL-7B* [1] to analyze the differences between the transferred frames and the original sequence. The model then revises the captions to more accurately reflect the updated visual semantics, as illustrated in Fig. 9.



Please revise the following caption so that it accurately matches the visual content and semantic context of the given image. Ensure the caption maintains a consistent style and tone with other video captions, describing what is happening in the image in a natural and coherent way.

Caption: The video depicts a 3D animated scene featuring a dragon perched atop a large, irregularly shaped rock formation. The dragon is rendered in grayscale, giving it a monochromatic appearance that emphasizes its form and structure. Its wings are spread wide, suggesting readiness for flight or perhaps a moment of rest after taking off ...




The video showcases a 3D animated scene where a majestic dragon is perched atop a large, irregularly shaped **rock** formation. The dragon is depicted in vibrant **orange** hues, with its wings spread wide, suggesting either readiness for flight or a moment of rest after taking off. **The rock formation is lush and green**, with **cascading waterfalls** flowing down its sides, creating a serene and mystical atmosphere ...

Figure 9. **Caption Refinement via MLLM.** Given a new first-frame image and its original caption, we use Qwen-2.5-VL to refine the caption so that the prompt for video generation more accurately matches the visual content and remains stylistically consistent with the input image.

7.3. Model Configuration.

We provide additional implementation details of our LongVie model. During training, we apply *input-frame degradation* with a probability of 20%. Within this process, VAE-based degradation is selected 20% of the time, while *generation degradation* is used for the remaining 80%. For encoding degradation, the parameter k is sampled from $[0, 10]$, with smaller values assigned higher sampling probability to simulate stronger degradation. For generation degradation, we select $t \in \{1, 5, 8, 10, 12\}$, again with a probability distribution favoring smaller values to emulate more severe degradation levels. In Stage 3, when history context is introduced, we apply the same degradation strategies to ensure consistent robustness across both current-frame and history-frame inputs.

In addition to frame-level degradation, we set the feature-level degradation probability α to 15% and the data-level degradation probability β to 10%. At each training step, one or both degradation types are randomly activated. We adopt a fusion count of $n = 5$ for the *Random Scale Fusion* module. To stabilize training, all degradation strategies are disabled during the first 2000 iterations and are gradually

introduced during the final 1000 iterations.

For weight initialization, the dense and sparse branches within each MM Block inherit only half of the original weights from Wan2.1 [40]. Specifically, we interleave the pretrained weights by index—assigning weights at positions $(0, 2, 4, \dots)$ to the dense branch and those at positions $(1, 3, 5, \dots)$ to the sparse branch—while simultaneously halving the feature dimensionality. This “half-copy” initialization substantially reduces the total parameter count and provides a stable starting point for joint dense–sparse control learning.

8. LongVGenBench

To better contextualize our proposed evaluation dataset, **LongVGenBench**, which is designed to assess both controllability and long-term quality and coherence in video world models, we present several representative examples in Fig. 10. The dataset consists of diverse real-world and synthetic scenes, each lasting at least one minute and captured at a minimum resolution of 1080p. As illustrated in the figure, LongVGenBench encompasses a wide range of camera motions, presenting substantial challenges for existing video generation models. Notably, the dataset is model-agnostic and can be used to evaluate any long-horizon video world model, not only LongVie. In this paper, we utilize LongVGenBench by splitting each video into 81-frame clips with a one-frame overlap, followed by extracting captions and control signals for each clip. These short-clip captions are then used to construct the corresponding inference data.

9. Additional Ablation Studies

Ablation for Degradation To further validate the effectiveness of our degradation strategy, we perform ablation studies on two degradation types: *Encoding Degradation* and *Generation Degradation*. The corresponding results are presented in Tab. 5. These experiments demonstrate the contribution of each component to our overall frame degradation training pipeline and highlight their complementary effects.

10. More Qualitative Results

To further demonstrate the robustness and versatility of our LongVie model, we provide additional qualitative results across multiple long video generation scenarios, including 1-minute, 3-minute, and 5-minute cases. These examples highlight the model’s ability to maintain high visual quality, preserve global consistency, and adapt to diverse styles over extended temporal horizons.

1-minute Cases. For the 1-minute videos, we showcase two representative settings: (1) a subject-driven scenario (a person riding a horse), and (2) a subject-free scenario captured from a drone perspective. Both settings are evaluated under three seasonal style transfers. As illustrated in Fig. 11 and Fig. 12, LongVie consistently preserves scene layout, motion

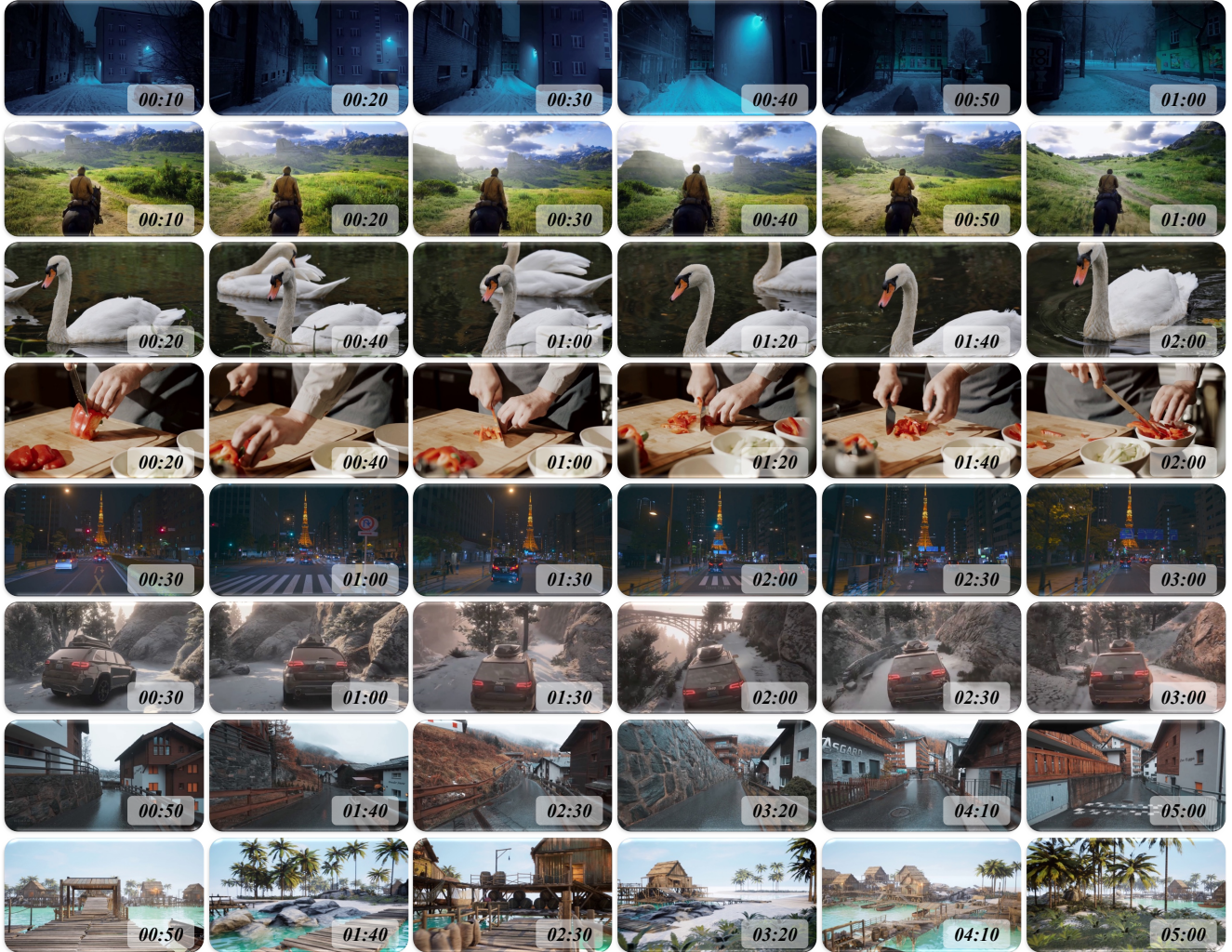


Figure 10. **Examples from LongVGenBench.** We show several videos from both real-world and synthetic scenarios in LongVGenBench, covering a variety of indoor and outdoor environments to evaluate the controllable long video generation ability of our model.

Table 5. **Ablation on the Degradation training of LongVie.** We progressively introduce three stages: *Control Learning*, *Degradation Adaptation*, and *History Context*. Each stage consistently enhances visual quality, controllability, and long-term consistency.

TRAINING STRATEGY	Quality		Controllability		Temporal Consistency			
	A.Q.↑	I.Q.↑	SSIM↑	LPIPS↓	S.C.↑	B.C.↑	O.C.↑	D.D.↑
Base Model	49.72%	63.78%	0.406	0.488	83.56%	88.86%	20.30%	15.15%
+ <i>Encoding Degradation</i>	52.18%	64.95%	0.451	0.402	85.72%	89.63%	20.66%	47.38%
+ <i>Generation Degradation</i>	53.96%	65.87%	0.478	0.356	87.64%	90.74%	21.14%	62.14%
+ <i>Both</i>	54.08%	66.21%	0.501	0.328	88.12%	91.05%	21.56%	76.12%

dynamics, and semantic integrity while accurately adapting global textures, lighting, and seasonal atmospheres across different styles.

3-minute Cases. For the 3-minute scenarios, we evaluate long-term consistency under seasonal style variations. As shown in Fig. 13, LongVie maintains coherent scene semantics and smooth transitions across all three seasonal styles.

5-minute Cases. To highlight LongVie’s capability in ultra-long video generation, we present two 5-minute examples covering both a subject-driven and a subject-free scenario. As shown in Fig. 14, LongVie preserves global structure, maintains coherent motion behavior, and sustains stable visual appearance throughout the entire 5-minute duration.

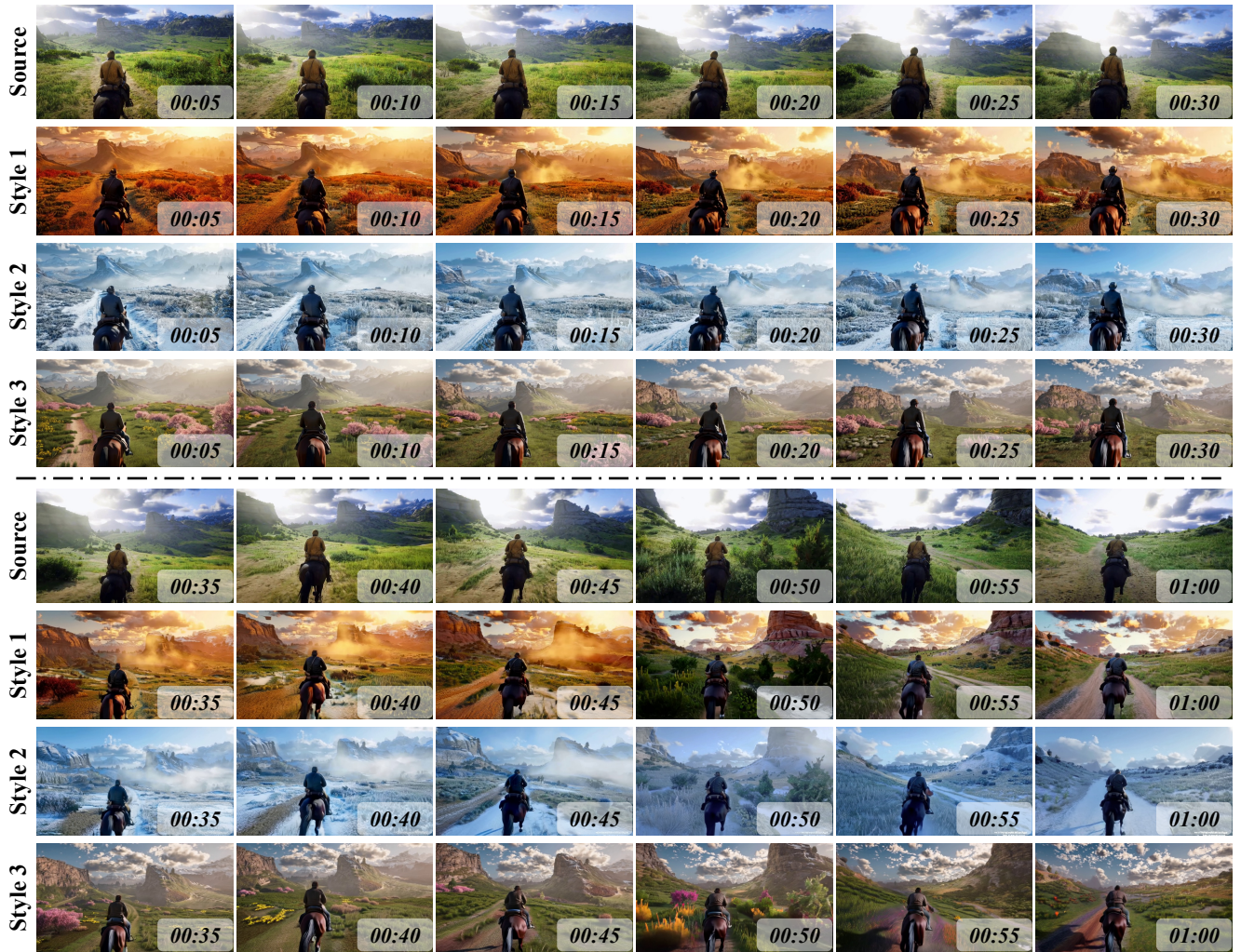


Figure 11. **Subject-driven 1-minute scenario.** A man riding a horse, transferred into multiple seasonal styles while preserving motion dynamics and scene structure.

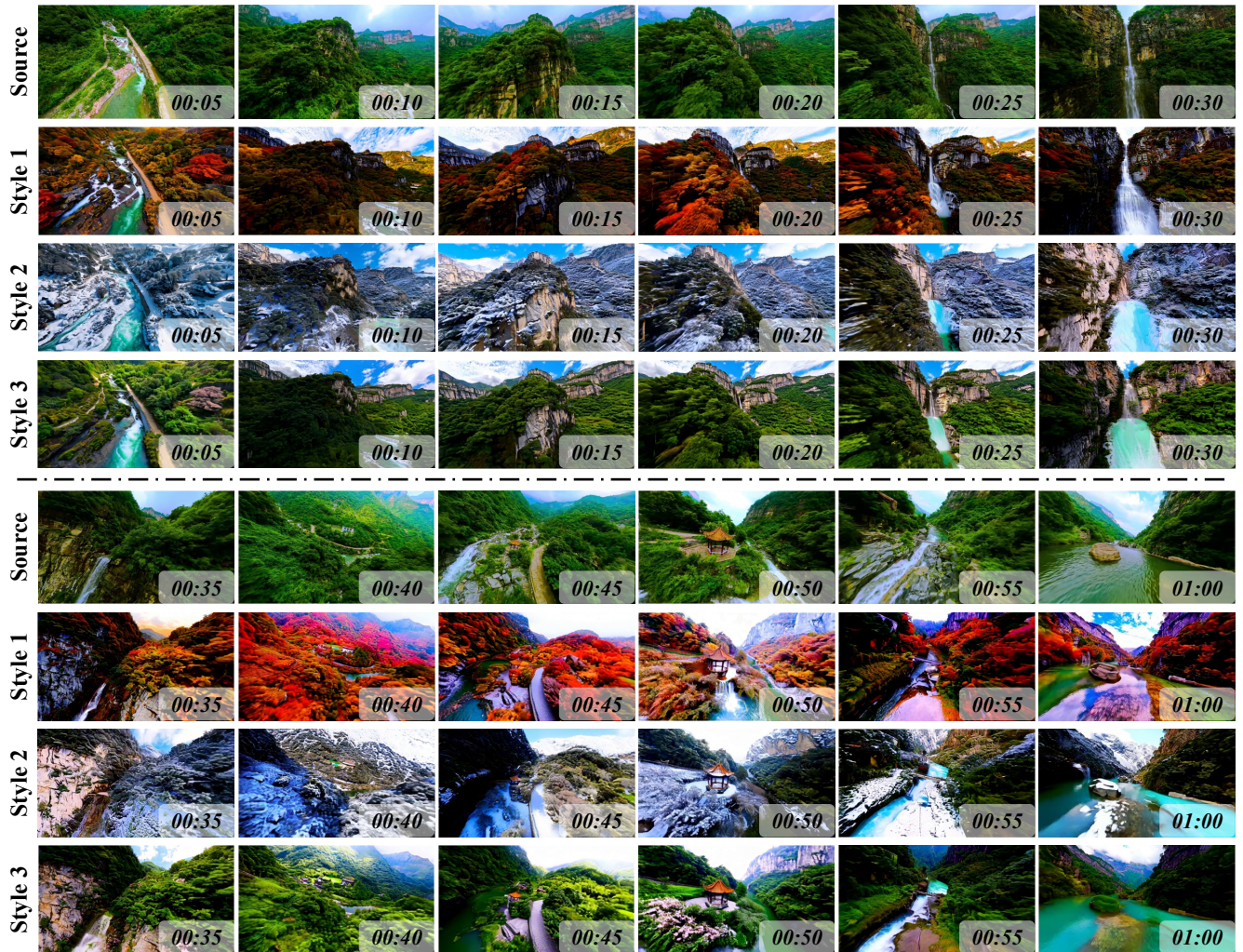


Figure 12. **Subject-free scenario.** A drone-like car-drive sequence through a mountain valley, transferred across different seasonal styles with consistent global appearance.

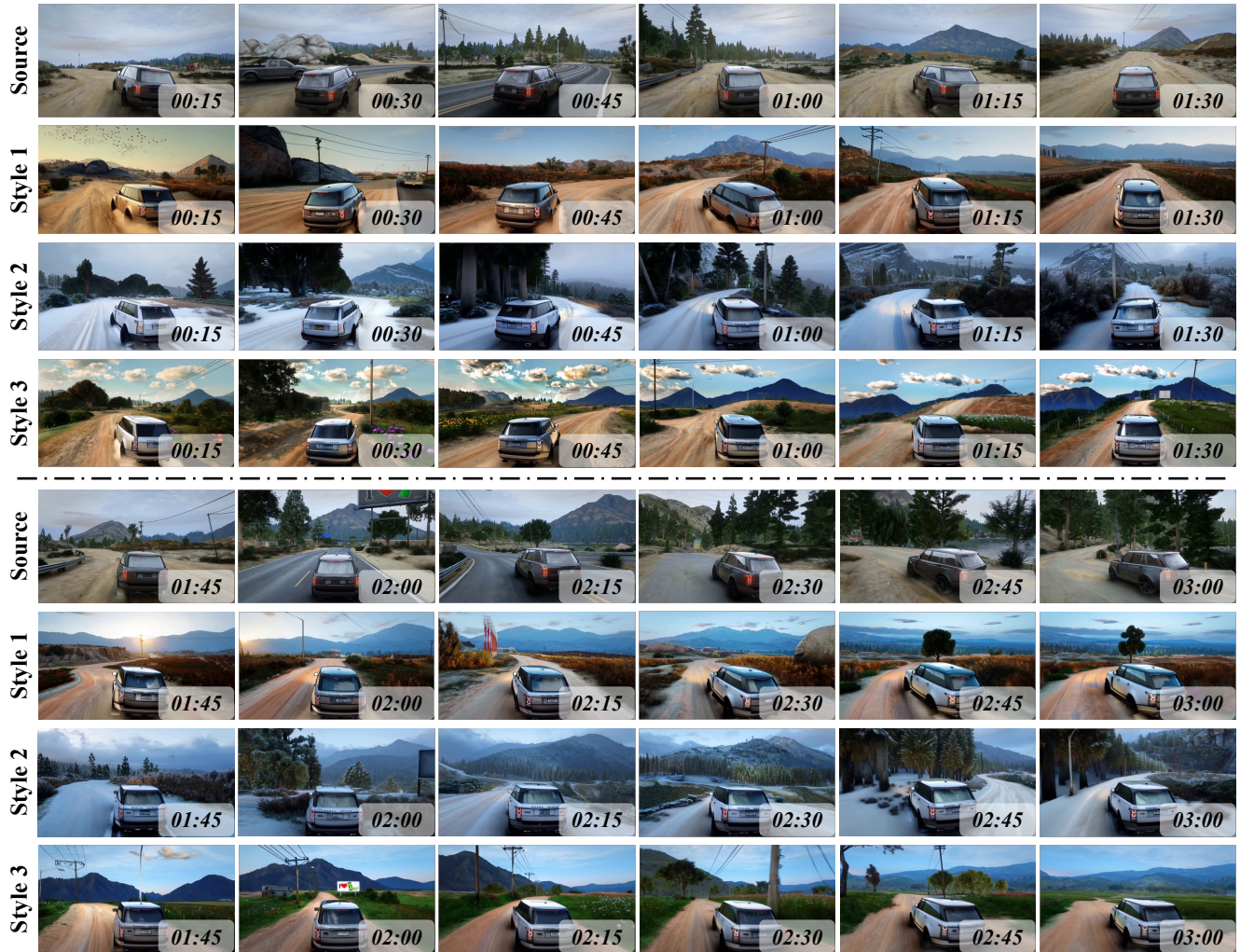


Figure 13. **3-minute scenario.** A car driving through a mountain valley is transferred into multiple seasonal styles, demonstrating LongVie’s ability to maintain long-range temporal consistency and coherent global appearance over extended durations.

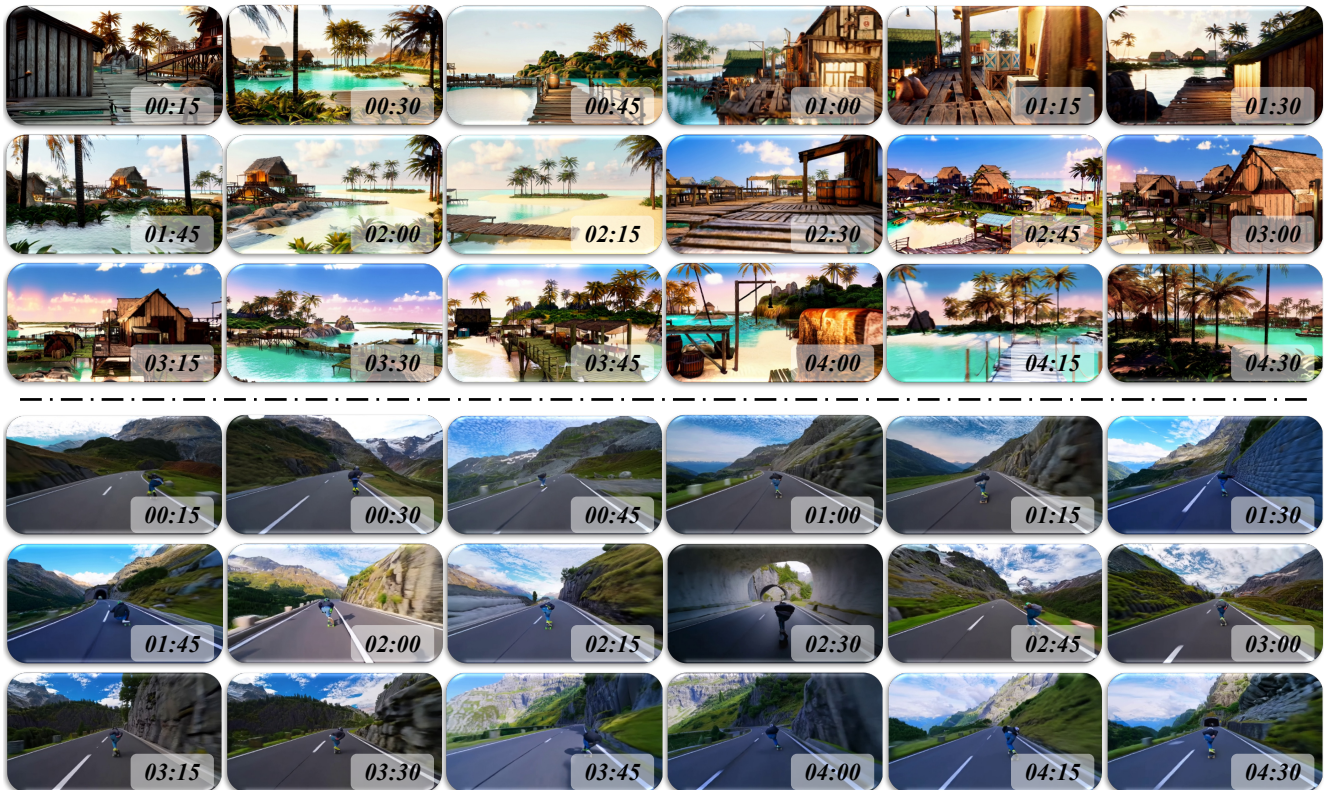


Figure 14. **5-minute scenarios.** We present two ultra-long video cases: a subject-driven sequence and a subject-free sequence. These results illustrate LongVie’s robustness in preserving structural stability, motion coherence, and style consistency across 5-minute continuous generations.

11. Limitations and Future Work

LongVie presents a practical framework for adapting a pre-trained video model into a controllable world model capable of generating coherent visual dynamics over 3–5 minutes. To systematically evaluate our training strategies while keeping computational costs tractable, all experiments in this paper are conducted at a resolution of 352×640 . Although this setting allows for comprehensive ablations and long-horizon testing, the relatively low resolution limits the model’s ability to express fine-grained details and high-frequency structures. In future work, we aim to scale LongVie to higher resolutions in order to further improve visual fidelity, capture richer scene dynamics, and more fully showcase the potential of LongVie as a video world model.